

## Original Paper

# Preparation of Kaolin Composites and Its Adsorption for Sb(III)

Wenxiang Luo<sup>1</sup>, Lu Tang<sup>1</sup>, Pan Zhang<sup>1</sup> & Chunyan Lang<sup>1\*</sup>

<sup>1</sup> College of Materials and Chemistry & Chemical Engineering, Chengdu University of Technology, Chengdu, Sichuan 610059, China

\* Corresponding author, Chunyan Lang, College of Materials and Chemistry & Chemical Engineering, Chengdu University of Technology, Chengdu, Sichuan 610059, China

Received: August 29, 2023 Accepted: September 24, 2023 Online Published: September 27, 2023

doi:10.22158/asir.v7n4p41

URL: <http://doi.org/10.22158/asir.v7n4p41>

### Abstract

Antimony is an important element in the production of flame retardants and semiconductor materials. In the process of antimony mining, it may cause local environmental pollution, which has adverse effects on human health, and the development of economical and efficient adsorbents to remove antimony from wastewater has become a hot research topic. In this paper, the hydrothermal synthesis method was adopted, and purified Kaolin was selected as the carrier, potassium permanganate, manganese chloride and ferric chloride are the metal sources, urea is the precipitant, and sodium dodecyl benzene sulfonate is the structure guide agent. Under the conditions of 5% mass fraction of dispersant, loading temperature of 140 °C, reaction time of 8 h, mass ratio of iron to manganese of 1.84:1, and mass of precipitant of 0.9 g, the composites prepared were effective in adsorbing the Sb(III) from the wastewater. The optimum adsorption efficiency of the prepared composites on Sb(III) is 92.83%, which showed excellent adsorption performance.

### Keywords

Antimony, Kaolin, Iron and manganese oxides, Adsorbent

## 1. Introduction

Antimony is a group of metallic elements with a wide range of industrial applications and is an important component of flame retardants, semiconductor materials, slide bearings and welding agents. However, antimony pollution caused by antimony mining and other activities has also become an environmental issue of global concern (Nishad & Bhaskarapillai, 2021). Antimony often exists in the form of inorganic antimony or organic antimony in natural water environment, in which the order of toxicity of antimony is Sb(III) > Sb(V) > Sb(Org). The Sb(III) form is often found in reductive water bodies and is relatively stable. Antimony in the environment can be accumulated in living organisms

through the food chain, and the antimony compounds formed can easily combine with sulfhydryl groups to inhibit enzyme activity and disrupt intracellular ionic equilibrium, which poses a great danger to the health of animals, plants, and human beings, and is regarded by the International Agency for Research on Cancer (IARC) as potentially carcinogenic to human beings (Fu, Xie, Charlet, & He, 2023). Therefore, the removal of antimony from wastewater is of great significance to environmental protection and human health (Deng, Ren, Hou, Deng, & Cheng, 2023).

At present, the main methods for removing antimony from wastewater are: ion exchange method, adsorption method, electrochemical method, chemical precipitation method and biological method (Dündar, Mehenktaş, & Arar, 2022; Peng, Wang, Xiao, Wang, Quan, Fu, Kong, & Zhang, 2023; Ren, Zheng, Li, & Liu, 2023; Wang, Chen, Mu, Zhang, Pan, Lee, & Chang, 2013; Wang, Wang, Ma, Zhang, Lyu, & Chen, 2022). However, most of these methods have many drawbacks such as environmentally unfriendly, low efficiency, high cost, and complicated process. In contrast, the adsorption method has been widely adopted due to many advantages such as high efficiency, low cost and environmental friendliness. The preparation of an efficient adsorbent has become a research hotspot. Clay minerals are widely used in the remediation of water pollution due to their loose and porous structure showing good adsorption properties, and they are a kind of adsorption material with great potential for development (Zhou, Zhao, Wang, Chen, & He, 2016). Common clay minerals are represented by bentonite, montmorillonite, bumpy clay, Kaolin and seafoam, etc. However, the surfaces of these natural clay minerals are negatively charged due to the presence of hydroxyl groups, and Sb(III), which exists in the form of acid radicals in the water column, is also negatively charged (Zhang, Ding, Gong, Deng, Huang, Zheng, Xiong, Tang, Wang, & Su, 2021). The adsorption effect of clay minerals on antimony is adversely affected. Therefore, natural minerals need to be modified to make them easily bind to antimony.

For example, the bacterial-mediated removal of antimony from water using Kaolin composite iron-manganese oxide (Xu, Li, Nan, Jiang, Wang, Xiong, Yang, Xu, & Jiang, 2022) achieved good adsorption results, but there are problems such as complicated experimental operation and possible environmental pollution of raw materials. There is also a simpler hydrothermal synthesis method (Du, Zhen, Wang, Ma, Wu, & Dai, 2022), seafoam as a carrier, loaded with iron and manganese oxides, the process is simple and environmentally friendly, the composite materials prepared for As(V) showed excellent adsorption performance. Arsenic and antimony are elements of the same main group with similar chemical behavior (Dousova, Lhotka, Buzek, Cejkova, Jackova, Bednar, & Hajek, 2020). Moreover, Sb(III) can be rapidly oxidized to Sb(V) under the action of manganese dioxide, and it is known in the literature that Sb(V) can be strongly adsorbed on various types of iron oxide in the form of intra-sphere bidentate binuclear complexes (Liu, Wang, Xiang, Wu, Yan, Zhang, Lin, & Chai, 2023), with a decrease in antimony content in the solution. Meanwhile, Kaolin is structurally similar to seafoam and is a typical layered silica-aluminate mineral with layers connected by hydrogen bonding

and a loose and porous structure with a large specific surface area, making it an excellent adsorbent material (Iji, Ibrahim, Argungu, & Obada, 2023).

Therefore, in this paper, hydrothermal synthesis method was adopted, Kaolin was selected as the carrier, loaded with iron-manganese oxide. And the preparation conditions were systematically optimized to obtain efficient adsorbent materials which can provide a part of the data support for the removal of Sb(III) from wastewater.

## 2. Experimental Section

### 2.1 Materials and Reagents

Kaolin (purchased from Xiangtan, Hunan Province, China); potassium antimony tartrate, sodium pyrophosphate, potassium permanganate, manganese chloride, ferric chloride, sodium dodecylbenzene sulfonate and urea were purchased from Chengdu Kolon Chemical Industry Co. Main.

Main instruments: oven (JZG-9070A, Changzhou Henglong Co., LTD.), high speed centrifuge (KH19A, Chengdu Xinyi Instrument Co., LTD.), hydrothermal reactor (KH-100mL, Shanghai Xiniu Leber Co., LTD.), Atomic fluorescence spectrometer (AFS-1790, Zhejiang Fuli Analytical Instruments Co., LTD.)

Sb(III) standard reserve solution ( $1.000 \text{ mgL}^{-1}$ ): weigh 2.7140 g of antimony potassium tartrate dissolved in deionized water, transferred to 1000 mL volumetric flask and fixed volume, to get  $1.000 \text{ mgL}^{-1}$  of Sb(III) reserve solution (other concentrations were diluted as needed for the experiment).

### 2.2 Preparation of Materials

#### 2.2.1 Purification of Kaolin

Take a certain amount of sodium pyrophosphate in 1L of ultrapure water, stirring at  $45 \text{ }^\circ\text{C}$  for 30 min, add 50 g of Kaolin, continue stirring for 1h and then leave it for 30 min, take the upper layer of the suspension and wash by centrifugal washing to pH neutral.  $85 \text{ }^\circ\text{C}$ , dry, grind and then pass through a 200 mesh sieve, bagged it and reserved it.

#### 2.2.2 Thermal Activation of Kaolin

The Kaolin with better adsorption effect after purification was respectively held in a muffle furnace at  $200\text{--}500 \text{ }^\circ\text{C}$  for 2 h to make heat-activated Kaolin, bagged it and reserved it.

#### 2.2.3 Acid and Thermal-acid Activation of Kaolin

Take the purified Kaolin with good adsorption effect and heat-modified Kaolin 3.0 g and add it into  $2.0\text{--}12.0 \text{ molL}^{-1}$  hydrochloric acid 30 mL, oscillate at  $65 \text{ }^\circ\text{C}$  for 3 h. After centrifugation, pour off the supernatant, wash the bottom product to neutral after cooling, dry it at  $85 \text{ }^\circ\text{C}$ , grind it and then pass it through a 200-mesh sieve, bagged it and reserved it.

#### 2.2.4 Preparation of Kaolin Loaded with Iron Oxide, Manganese Oxide and Iron-manganese Oxide

Kaolin loaded with iron oxide, manganese oxide and iron-manganese oxide: Weigh 1.0 g of purified Kaolin, heat activated Kaolin, acid activated Kaolin and heat-acid activated Kaolin, which had the best adsorption effect on Sb(III), dispersed in 20 mL ultrapure water, stirred thoroughly. Add the same

quality of sodium dodecyl benzene sulfonate, urea, different quality of ferric chloride, manganese chloride and potassium permanganate, transfer the mixed solution to the hydrothermal reactor, reaction at the same temperature for the same time. After the reaction product is cooled to room temperature, washed with deionized water to neutral, dried at 60 °C, ground through a 200-mesh sieve, bagged and sealed for storage.

Optimization of preparation conditions : Weigh 1.0 g of the best pretreatment effect of a certain type of Kaolin, dispersed in 20 mL of ultrapure water, stirred thoroughly; add 0.12 g of sodium dodecyl benzene sulfonate, and then add a different quality of urea (0.6~4.5 g), change the mass ratio of iron, manganese (0.92:1~4.52:1), transfer the mixed solution to a hydrothermal reactor, and the reaction was carried out for a number of hours (2~14 h) at different temperatures (120~200 °C). The reaction products were cooled to room temperature, washed with deionized water to neutral, dried at 60 °C, ground through a 200-mesh sieve, and sealed in bags for storage.

The process of treating Kaolin in different ways is shown in Figure 1.

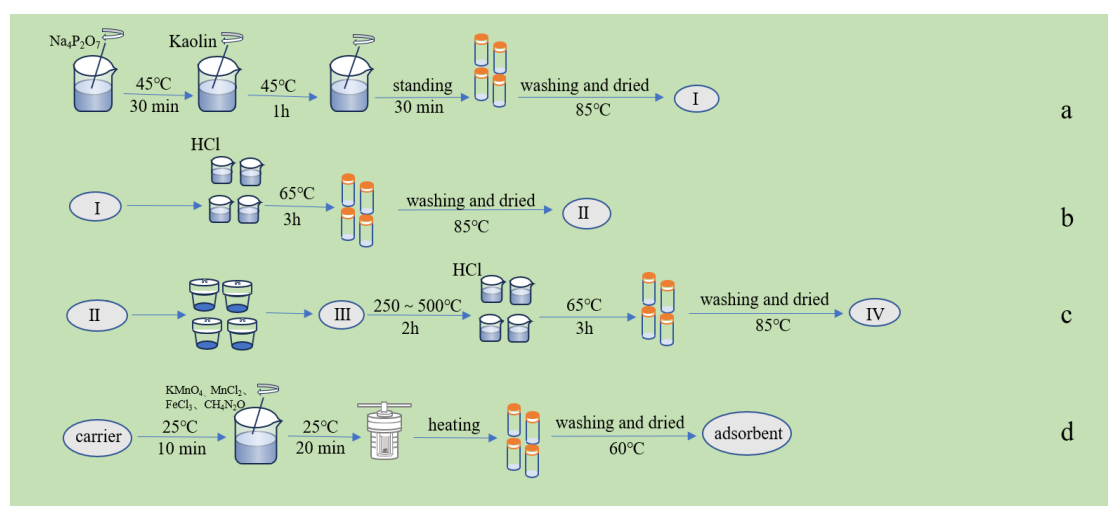


**Figure 1. Preparation of Kaolin Adsorbent Materials by Different Treatments**

**a. Purification. b. Acid Activation. c. Thermal-acid Activation. d. Fabrication.**

### 2.3 Adsorption Experiment

To 25 mL of Sb(III) adsorption solution, 100 mg of adsorbent was added separately, and the adsorption reaction was carried out at a temperature of 25 °C, pH = 7, and an initial concentration of Sb(III) of 20 mg·mL<sup>-1</sup> for 2 h. The concentration of Sb(III) in the equilibrium solution was determined by atomic fluorescence method at the end of the reaction. The adsorption efficiency  $\eta$  (%) is calculated according to equations (1).

$$\eta = \frac{c_0 - c_e}{c_0} \times 100\% \quad (1)$$

where  $C_0$  and  $C_e$  are the initial and equilibrium concentrations of Sb(III) (mg·L<sup>-1</sup>), respectively.

### 3. Results and Discussion

#### 3.2 Adsorption Efficiency of Several Processed Kaolin for Sb(III)

The adsorption of antimony (III) was carried out with purified Kaolin, heat activated, acid activated and heat-acid activated Kaolin, respectively, and the results are shown in Figure 2.

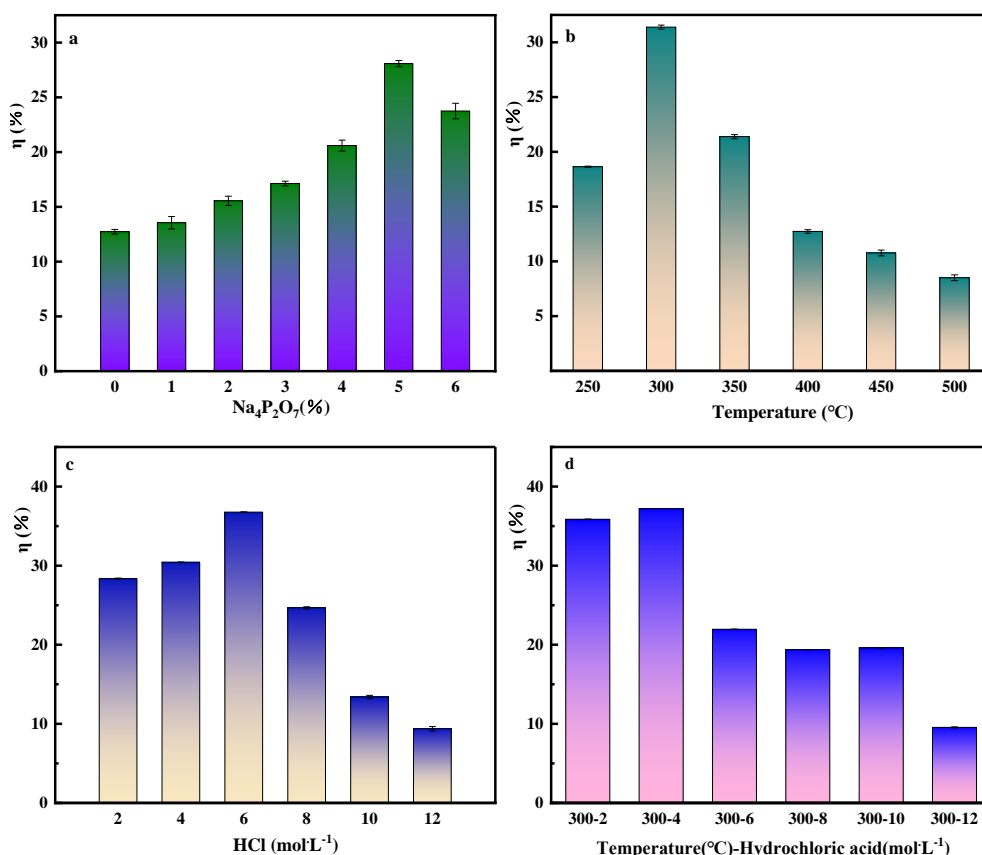


**Figure 2. Adsorption Efficiency of Several Processed Kaolin for Antimony (III)**

**a. Purification. b. Thermal Activation. c. HCl. d. Thermal-acid Activation.**

As can be seen from Figure 2a, the adsorption effect of purified Kaolin on Sb(III) was gradually enhanced by increasing the dosage of sodium pyrophosphate, and the adsorption rate was maximum when the dosage of sodium pyrophosphate was 5%, and the adsorption rate began to decrease when the dosage of sodium pyrophosphate continued to increase. This is because sodium pyrophosphate, as a dispersant, can play a role in reducing the friction coefficient of the Kaolin surface and increasing its surface energy (Nadiv, Vasilyev, Shtein, Peled, Zussman, & Regev, 2016), and also dredge the internal pores of the ore, remove internal symbiotic impurities, increase the adsorption sites and improve the adsorption effect. However, when the optimal dosage is exceeded, the excess sodium pyrophosphate will accumulate in the lamellar structure of Kaolin, blocking some of the pore channels and reducing the effective active adsorption sites, and the adsorption rate of Sb(III) by Kaolin is thus reduced.

From Figure 2b, it can be seen that the adsorption rate gradually increased with the increase of roasting temperature, which was attributed to the appropriate increase in temperature, the adsorbed water and water of crystallization content in the Kaolin decreased (Xie, Ni, Han, Zhong, He, & Sun, 2023), and the pore volume and the specific surface area of the Kaolin increased; when the temperature was increased to 300 °C, the adsorption rate reached the maximum; the temperature continued to increase, the pore structure would begin to collapse, and the adsorption capacity of Kaolin on Sb(III) decreased (Feng, Kou, Tang, Shi, Tong, & Zhang, 2023).

As can be seen from Figure 2c and Figure 2d, hydrochloric acid with concentrations of 6 mol·L<sup>-1</sup> and 4 mol·L<sup>-1</sup> had the best effect on the thermal activation of purified Kaolin and 300°C heat-activated Kaolin. This is because a certain concentration of acid can remove impurities such as metal ions and other inorganic substances such as Mg(II) and Al(III) on the surface of the ore, increase the specific surface area of the ore, unclog the pore channels and increase the adsorption capacity (Española, Sarkar, Biswas, Rusmin, & Naidu, 2019). With the increase of acid concentration, the silica hydroxyl group on the surface of Kaolin decreases, the surface structure of the ore changes and becomes rougher, the specific surface area decreases, while the internal structure collapses, the pores are blocked, and the adsorption rate decreases as a result (Song, Mahy, Calberg, Farcy, Caucheteux, Fagel, & Lambert, 2023).

### 3.3 Effect of Preparation Conditions on the Adsorption of Sb(III) by Composites

#### 3.3.1 Adsorption of Sb(III) by Different Pretreatment Kaolin Loadings Alone and Mixed Iron and Manganese Oxides

Based on the experimental results of 3.1, the Kaolin with the best adsorption effect on Sb(III) of four kinds of Kaolin was selected as the carrier, loaded with iron oxide (I-Kaolin), manganese oxide (M-Kaolin) and iron-manganese oxide (IM-Kaolin), respectively, and the composites with the best adsorption effect on Sb(III) were selected after comparison of adsorption effects, and the results are shown in Figure 3.

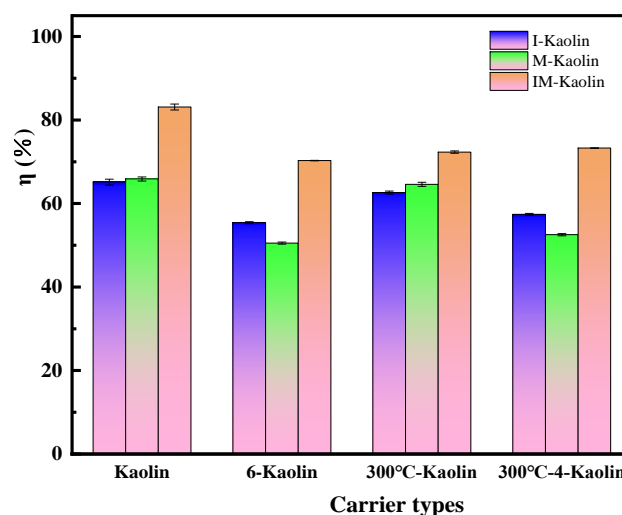


**Figure 3. Four Pretreated Kaolin Loaded with Different Substances**

The results show that among the four kinds of Kaolin treated with different pretreatment, the purified Kaolin had significantly better adsorption effect on antimony(III) than acid-activated, thermally-activated and thermo-acid-activated Kaolin. This is because the internal structure of the purified Kaolin was least affected. When the metal oxide was loaded, the metal oxide could grow uniformly on its surface, and the covered area of the metal oxide was larger. There are more effective metal oxides loaded on the surface of Kaolin. The results also show that Kaolin loaded with iron-manganese oxide showed the higher adsorption efficiency of Sb(III), compared with Kaolin loaded with iron oxide and manganese oxide. This is because the manganese dioxide on the surface of the composite material can convert part of Sb(III) to Sb(V) and reduce antimony toxicity, as well as provide more active adsorption sites for the material to adsorb Sb(III). The adsorption efficiency of purified Kaolin for antimony(III) can reach 82.62%.

### 3.3.2 Optimization of Composite Preparation

According to the results of 3.2.1, purified Kaolin was selected as the carrier to synthesize the composites and optimize the preparation conditions, and the experimental results are shown in Figure 4.

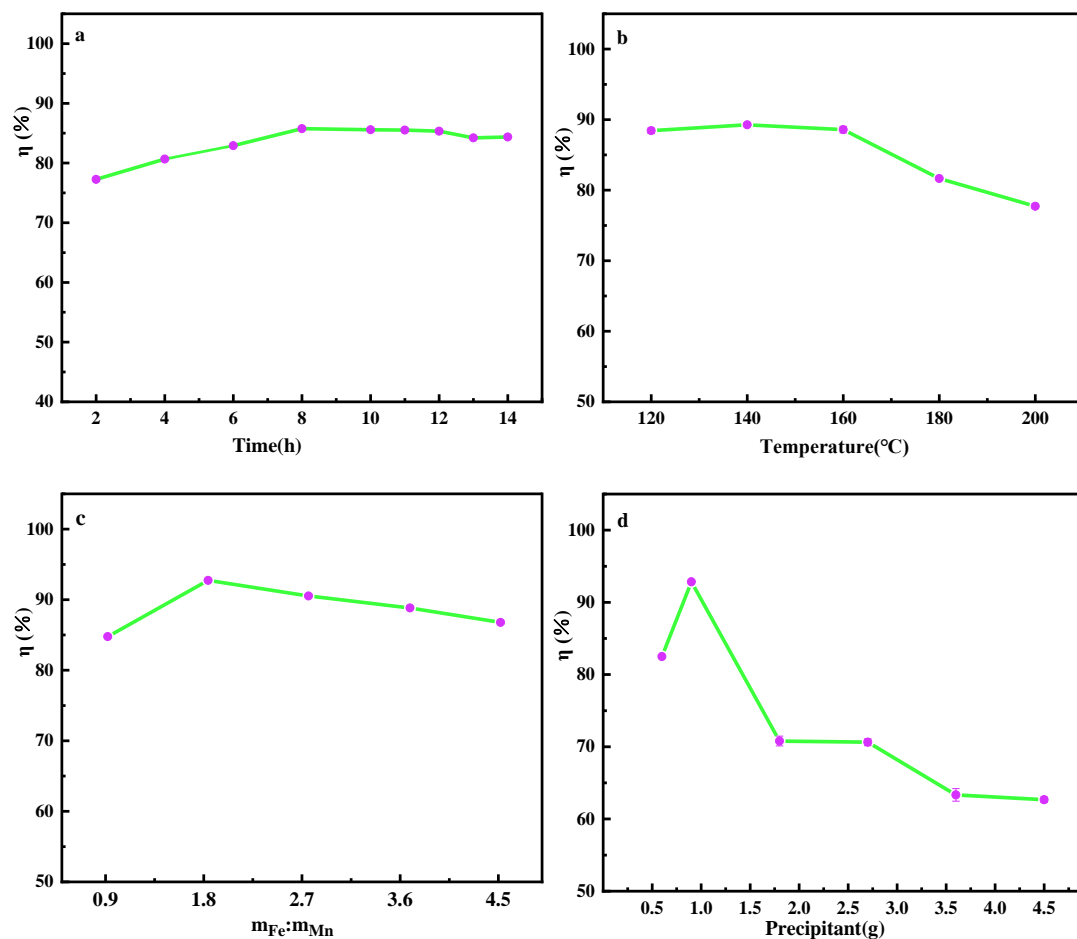


**Figure 4. Optimization of Composite Preparation Conditions**

**a. Time. b. Temperature. c.  $m_{Fe}:m_{Mn}$ . d. Precipitant**

As can be seen from Figure 4a, when the hydrothermal reaction time is lower than 8 h, the adsorption rate is enhanced with the increase of time, and after the reaction time is higher than 8 h, the increase of time does not have much effect on the adsorption rate. It indicates that when the hydrothermal reaction time reaches 8 h, the iron-manganese oxide has completely realized the uniform growth on the surface of Kaolin, and the iron-manganese oxide has completely encapsulated the Kaolin, and at this time, the adsorption efficiency of the composites on Sb(III) is 85.85%. Prolonging the hydrothermal reaction time, there will not be more iron-manganese oxide precipitated to the surface of Kaolin, and the adsorption effect of the composite material on Sb(III) is basically stable and no longer undergoes great changes.

As can be seen from Figure 4b, the adsorption rate of Sb(III) of the prepared composites was higher and more stable at the hydrothermal reaction temperature of 120~160 °C; the best adsorption effect was achieved at a temperature of 140 °C; the adsorption efficiency decreased when the temperature was more than 140 °C, which may be due to the fact that too high a temperature of the hydrothermal reaction would lead to the deformation of the Kaolin carriers dispersed in the solution or the sintering of the iron-manganese oxide, which The crystallinity decreased, which reduced its adsorption efficiency. The adsorption efficiency of the composite material for Sb(III) was 89.42% at the hydrothermal reaction temperature of 140 °C.

As can be seen from Figure 4c, the highest adsorption rate of Sb(III) for the composite was 92.78% when the mass ratio of iron and manganese was increased to 1.84 : 1 during the composite preparation. This is because the iron oxide can form a complex with antimonate, which plays a major role in the adsorption process, and when the mass ratio of iron and manganese gradually increases, the iron content also gradually increases. At this time, the loading sites on the Kaolin slowly reached saturation; When the mass ratio of iron to manganese is 1.84:1, and iron and manganese oxides are completely wrapped on the surface of Kaolin. If the ratio was continued to be increased, the iron-manganese oxide hydroxide would block the pore size and sites on the Kaolin, and the adsorption efficiency would decrease.

As can be seen from Figure 4d, when the precipitant urea was added with a mass of 0.9 g, the prepared composites showed the best adsorption effect on Sb(III), and it was inferred that under this condition, Kaolin and iron-manganese oxide had been completely combined, and by continuing to increase the mass of the precipitant, the solution pH became high and the surface of the matrix became negatively charged, which was not conducive to the adsorption of Sb(III). And when the urea was less than 0.9 g, the iron-manganese oxide was not able to completely precipitate on the surface of Kaolin, which affected the adsorption of Sb(III). The adsorption efficiency of the composite for Sb(III) was 92.83% when the mass of precipitant was 0.9 g.

#### 4. Conclusion

In this paper, four kinds of Kaolin with the best adsorption effect on Sb(III) were selected from purified Kaolin, heat-activated Kaolin, acid-activated Kaolin and heat-acid activated Kaolin, respectively. And



by using the hydrothermal reaction method, the four types of Kaolin were loaded with iron oxide, manganese oxide and iron-manganese oxide, respectively. The results showed that the composites with purified kaolin as the carrier loaded with iron-manganese oxide had the best adsorption effect on Sb(III). And optimized the preparation conditions, the composites showed that the highest adsorption rate of Sb(III) was up to 92.83%. In summary, the composite prepared in this paper has reached the expected goal from the experimental point of view. These conclusions can provide certain data support and theoretical reference for antimony pollution control in water, which is conducive to reducing the potential harm of antimony to the environment.

## References

- Deng, S., Ren, B., Hou, B., Deng, R., & Cheng, S. (2023). Antimony-complexed heavy metal wastewater in antimony mining areas: Source, risk and treatment. *Environmental Technology & Innovation*, 32. <https://doi.org/10.1016/j.eti.2023.103355>
- Dousova, B., Lhotka, M., Buzek, F., Cejkova, B., Jackova, I., Bednar, V., & Hajek, P. (2020). Environmental interaction of antimony and arsenic near busy traffic nodes. *Science of The Total Environment*, 702. <https://doi.org/10.1016/j.scitotenv.2019.134642>
- Du, Y., Zhen, S., Wang, J., Ma, Y., Wu, J., & Dai, H. (2022). FeOOH-MnO<sub>2</sub>/Sepiolite and Fe<sub>2</sub>O<sub>3</sub>-MnO<sub>2</sub>/Diatomite: Highly efficient adsorbents for the removal of As(V). *Applied Clay Science*, 222. <https://doi.org/10.1016/j.clay.2022.106491>
- Dündar, O. A., Mehenktaş, C., & Arar, Ö. (2022). Removal of Antimony(III) and Antimony(V) from water samples through water-soluble polymer-enhanced ultrafiltration. *Environmental Research*, 215. <https://doi.org/10.1016/j.envres.2022.114324>
- España, V. A. A., Sarkar, B., Biswas, B., Rusmin, R., & Naidu, R. (2019). Environmental applications of thermally modified and acid activated clay minerals: Current status of the art. *Environmental Technology & Innovation*, 13, 383-397. <https://doi.org/10.1016/j.eti.2016.11.005>
- Feng, M., Kou, Z., Tang, C., Shi, Z., Tong, Y., & Zhang, K. (2023). Recent progress in synthesis of zeolite from natural clay. *Applied Clay Science*, 243. <https://doi.org/10.1016/j.clay.2023.107087>
- Fu, X., Xie, X., Charlet, L., & He, J. (2023). A review on distribution, biogeochemistry of antimony in water and its environmental risk. *Journal of Hydrology*, 625. <https://doi.org/10.1016/j.jhydrol.2023.130043>
- Iji, J. O., Ibrahim, F. B., Argungu, A. S., & Obada, D. O. (2023). Development and optimization of hydroxyapatite/kaolin-based ceramic materials as potential adsorbents for water purification. *Environmental Advances*. <https://doi.org/10.1016/j.envadv.2023.100419>
- Liu, X., Wang, Y., Xiang, H., Wu, J., Yan, X., Zhang, W., Lin, Z., & Chai, L. (2023). Unveiling the crucial role of iron mineral phase transformation in antimony(V) elimination from natural water. *Eco-Environment & Health*, 2(3), 176-183. <https://doi.org/10.1016/j.eehl.2023.07.006>

- Nadiv, R., Vasilyev, G., Shtein, M., Peled, A., Zussman, E., & Regev, O. (2016). The multiple roles of a dispersant in nanocomposite systems. *Composites Science and Technology*, *133*, 192-199. <https://doi.org/10.1016/j.compscitech.2016.07.008>
- Nishad, P. A., & Bhaskarapillai, A. (2021). Antimony, a pollutant of emerging concern: A review on industrial sources and remediation technologies. *Chemosphere*, *277*. <https://doi.org/10.1016/j.chemosphere.2021.130252>
- Peng, L., Wang, N., Xiao, T., Wang, J., Quan, H., Fu, C., Kong, Q., & Zhang, X. (2023). A critical review on adsorptive removal of antimony from waters: Adsorbent species, interface behavior and interaction mechanism. *Chemosphere*, *327*. <https://doi.org/10.1016/j.chemosphere.2023.138529>
- Ren, Y., Zheng, W., Li, S., & Liu, Y. (2023). Atomic H\*-mediated electrochemical removal of low concentration antimonite and recovery of antimony from water. *Journal of Hazardous Materials*, *445*. <https://doi.org/10.1016/j.jhazmat.2022.130520>
- Song, P. N., Mahy, J. G., Calberg, C., Farcy, A., Caucheteux, J., Fagel, N., & Lambert, S. D. (2023). Influence of thermal and acidic treatments on the morphology of a natural kaolinitic clay mineral. *Results in Surfaces and Interfaces*, *12*. <https://doi.org/10.1016/j.rsurfi.2023.100131>
- Wang, H., Chen, F., Mu, S., Zhang, D., Pan, X., Lee, D.-J., & Chang, J.-S. (2013). Removal of antimony (Sb(V)) from Sb mine drainage: Biological sulfate reduction and sulfide oxidation-precipitation. *Bioresource Technology*, *146*, 799-802. <https://doi.org/10.1016/j.biortech.2013.08.002>
- Wang, Q., Wang, B., Ma, Y., Zhang, X., Lyu, W., & Chen, M. (2022). Stabilization of heavy metals in biochar derived from plants in antimony mining area and its environmental implications. *Environmental Pollution*, *300*. <https://doi.org/10.1016/j.envpol.2022.118902>
- Xie, Y., Ni, C., Han, Z., Zhong, H., He, Z., & Sun, W. (2023). High recovery of lithium from coal residue by roasting and sulfuric acid leaching. *Minerals Engineering*, *202*. <https://doi.org/10.1016/j.mineng.2023.108284>
- Xu, R., Li, Q., Nan, X., Jiang, G., Wang, L., Xiong, J., Yang, Y., Xu, B., & Jiang, T. (2022). Simultaneous removal of antimony(III/V) and arsenic(III/V) from aqueous solution by bacteria-mediated kaolin@Fe-Mn binary (hydr)oxides composites. *Applied Clay Science*, *217*. <https://doi.org/10.1016/j.clay.2021.106392>
- Zhang, Y., Ding, C., Gong, D., Deng, Y., Huang, Y., Zheng, J., Xiong, S., Tang, R., Wang, Y., & Su, L. (2021). A review of the environmental chemical behavior, detection and treatment of antimony. *Environmental Technology & Innovation*, *24*. <https://doi.org/10.1016/j.eti.2021.102026>
- Zhou, C. H., Zhao, L. Z., Wang, A. Q., Chen, T. H., & He, H. P. (2016). Current fundamental and applied research into clay minerals in China. *Applied Clay Science*, *119*, 3-7. <https://doi.org/10.1016/j.clay.2015.07.043>